Femtosecond Dynamics of the Ring Closing Process of Diarylethene: A Case Study of Electrocyclic Reactions in Photochromic Single Crystals

Cite as:
Morrison, C. (2011). Femtosecond Dynamics of the Ring Closing Process of Diarylethene: A Case Study of Electrocyclic Reactions in Photochromic Single Crystals. *Journal of Physical Chemistry A* , 115(45), 13158-13168.

Manuscript received: 21/06/2011; Accepted: 25/08/2011; Article published: 22/09/2011

Femtosecond dynamics of the ring closing process of diarylethene: A case study of electrocyclic reactions in photochromic single crystals**

Hubert Jean-Ruel,[1] Ryan R. Cooney,[1] Meng Gao,[1] Cheng Lu,[1] Michal A. Kochman,[2] Carole A. Morrison,[2] and R. J. Dwayne Miller[1,3,*]

[1]Departments of Chemistry and Physics, 80 St. George Street, University of Toronto, Toronto, Ontario, M5S 3H6, Canada.

[2]EaStCHEM, School of Chemistry, Joseph Black Building, University of Edinburgh, West Mains Road, Edinburgh, EH9 3JJ, UK.

[3]Max Planck Department for Structural Dynamics, Department of Physics, University of Hamburg, Centre for Free Electron Laser Science, DESY, Notkestrasse 85, Hamburg 22607, Germany.

[*]Corresponding author; e-mail: dwayne.miller@mpsd.cfel.de

[**]This work was supported by the Natural Sciences and Engineering Research Council of Canada (NSERC), the Canadian Foundation for Innovation, and the Ontario Research Foundation, and by the Centre for Numerical Algorithms and intelligent Software (funded by EPSRC grant EP/G036136/1 and the Scottish Funding Council). This work has also made use of the resources provided by the Edinburgh Compute and Data Facility (ECDF), (http://www.ecdf.ed.ac.uk/). The ECDF is partially supported by the eDIKT initiative (http://www.edikt.org.uk). H.J-R. and R.R.C. gratefully acknowledge support through a Vanier Fellowship and NSERC Postdoctoral Fellowship respectfully, and M.A.K. the University of Edinburgh for the award of a Principal's Career Development Scholarship. The authors thank Prof. Irie for early discussion on the photochemistry of diarylethenes and the generous gift of a crystal to help initiate this work.

Supporting information:
Supplementary material is available free of charge online at http://pubs.acs.org

Keywords:
Femtosecond transient absorption spectroscopy; Ultrafast electron diffraction; Vibrational mode analysis; Photochromism; Cyclization; Ultrafast spectroscopy of single crystal photochemistry

Abstract

The cyclization reaction of the photochromic diarylethene derivative 1,2-bis(2,4-dimethyl-5-phenyl-3-thienyl) perfluorocyclopentene was studied in its single crystal phase with femtosecond transient absorption spectroscopy. The transient absorption measurements were performed with a robust acquisition scheme which explicitly exploits the photoreversibility of the molecular system and monitors the reversibility conditions. The crystalline system demonstrated 3 x 10^4 repeatable cycles before significant degradation was observed. Immediately following photoexcitation, the excited state absorption associated with the open-ring conformation undergoes a large spectral shift with a time constant of approximately 200 fs. Following this evolution on the excited state potential energy surface, the ring-closure occurs with a time constant of 5.3 ps, which is significantly slower than previously reported measurements for similar derivatives in solution phase. Time resolved electron diffraction studies were used to further demonstrate the assignment of the transient absorption dynamics to the ring closing reaction. The mechanistic details of the ring closing are discussed in the context of prior computational work along with a vibrational mode analysis using density functional theory to give some insight into the primary motions involved in the ring closing reaction.

1. Introduction

Diarylethene derivatives are a family of photochromic compounds which are extensively studied because of their potential for fabricating photonic devices such as all-optical memories and switches[1,2], as well as nano- and micro-actuators[3,4]. Photochromism refers to the ability of certain molecules to undergo a photoinduced reaction between two isomers which have different absorption spectra. For the diarylethenes, the isomerization is a classic example of an electrocyclic reaction which involves the reversible ring-closing (cyclization) and ring-opening (cycloreversion) of the molecular system, following irradiation with UV and visible light, respectively. The ability of diarylethene derivatives to photoreversibly undergo subsequent cyclization and cycloreversion with large changes in optical properties is the key reason for their potential in fabricating photonic devices.

The fundamental requirements of a photochromic system for applications in all-optical memories and switches are that they be thermally stable in their variable state condition and fatigue resistance. Furthermore, technological applications will generally require a solid state system. The pioneering work of Irie *et al*.[1] has demonstrated that diarylethene derivatives with heterocyclic aryl groups satisfy these requirements. That is, both open- and closed-ring isomers have been shown to be stable even at 80 ^{O}C and to be capable of undergoing more than 10^4 ring-closing and ring-opening cycles before significant degradation is observed. Furthermore, several of these derivatives also exhibit photochromism in the crystalline phase[5], making them particularly promising candidates for technological applications. One such compound is 1,2-bis(2,4-dimethyl-5-phenyl-3-thienyl) perfluorocyclopentene (Scheme 1).

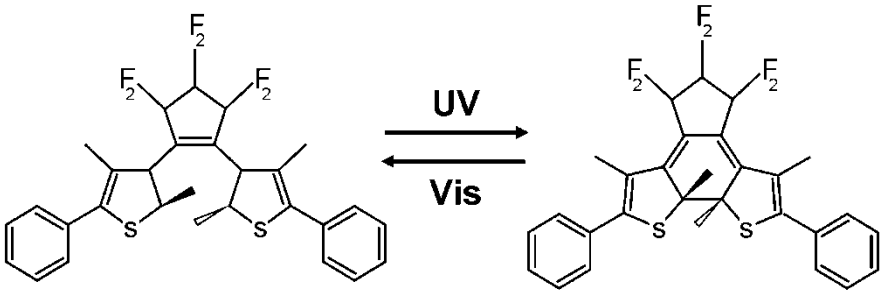

Scheme 1.

To determine the ultrafast dynamics of these systems associated with both the cyclization and cycloreversion reactions in various diarylethene derivatives a large number of time-resolved spectroscopic studies have been performed on these systems[6-29]. Not only do these studies offer insight on the general attributes of electrocyclic reactions, but they also reveal the speed of the ring-closing and ring-opening reactions which is the crucial aspect for both the quantum yield and the fatigue resistance, since these processes are, in general, in competition with other radiative and nonradiative relaxation channels. The comparison of the time constants for those reactions in different diarylethene derivatives, along with an understanding of the different reaction pathways involved, is essential for designing new compounds with increased performance.

Even though technological applications will generally require the solid state, the majority of ultrafast studies have been carried out in solution, with the general consensus that the cyclization occurs on sub-picosecond to picoseconds timescales[6-20]. Though solution phase measurements have the advantage of continuously flowing the sample such that complete reversibility of initial conditions is ensured for every transient absorption (pump-probe) event, the periodic crystal structure and intermolecular contacts associated with the solid state will presumably have some effect on the reaction pathways. The cyclization reaction requires the heterocyclic aryl moieties to undergo relatively large motions which increase the planarity of the closed ring isomer and aid the delocalization the π electronic structure[1,30,31]. When considering the crystalline phase, the surrounding matrix should influence these relatively large scale motions and alter the observed reaction dynamics. Only a limited number of time-resolved studies have been performed on diarylethene derivatives in their crystalline phase[8,18,27] and to our knowledge none were done with femtosecond resolution. Though these previous studies provide upper limits to the reaction time scale, they were limited to picosecond temporal resolution and were unable to fully characterize the cyclization reaction.

A fundamental requirement for all transient absorption experiments is that the sample under study fully recovers between laser shots in order to be in the same initial state for each pump-probe event. In principle, the solid state can be investigated even for nonreversible systems simply by translating the sample between excitation pulses. However, for the crystalline phase it is often non-trivial to create large area samples that can support adequate excitation area to reconstruct the dynamics with sufficient signal to noise. In this case, the

photoreversibility of diarylethene provides a major advantage to the study of photochemical reaction mechanisms in the solid state. That is, the photochromic properties make it possible, in principle, to perform femtosecond pump-probe measurements in the single crystal phase without constant exchange of sample. Specifically, the requisite reversibility can be met by following each pump-probe event resulting in cyclization with a second visible pump to revert the system back to its initial conditions. In addition, the thermal stability of the system can be exploited to systematically compare the transient signal with that of the final photoproduct. By measuring the steady-state absorption profile of the photoproduct associated with every transient pump-probe event the convergence to the closed-ring isomer can be monitored. More importantly, this exploitation of the systems thermal stability can be used to ensure that the sample is still in the photoreversible regime. That is, there is a limit to the total number of photon cycles that can be executed for a given spot, termed the fatigue resistance, and this point needs to be independently determined for the given excitation conditions.

Here we present femtosecond transient absorption measurements of the ring-closing reaction in the single crystal diarylethene derivative 1,2-bis(2,4-dimethyl-5-phenyl-3-thienyl) perfluorocyclopentene. These measurements were made by exploiting both the systems photoreversibility and thermal stability. To our knowledge, no previous study has made such direct and complete use of the photochromic capabilities of a diarylethene derivative for time-resolved measurements. These optical experiments are complemented by preliminary time-resolved electron diffraction results, and represent the first study where sufficient temporal resolution has been used to resolve the entire electrocyclic reaction of a diarylethene derivative in its single crystalline state. The methods employed here, and the exploitation of this system's photoreversibilty, make it tractable to work with small area single crystal samples and are particularly important for time resolved electron or X-ray diffraction studies where single crystals make it possible to directly observe the atomic motions coupled to the reaction coordinate[32]. This work paves the way for the use of femtosecond electron diffraction to directly determine the key atomic motions and time dependent velocities through reactive crossings to construct potential energy surfaces at the finest level of detail. Here we discuss the mechanistic details in the context of prior computational work[33] and offer a vibrational mode analysis to give some insight into the primary motions involved in the ring closing reaction.

2. Experimental and computational methods

The transient differential absorption (pump-probe) measurements were made with a home built Ti:sapphire oscillator and associated regenerative amplifier system (500 Hz, 810 nm, 50 fs, and 500 μJ). White light continuum was generated in a sapphire window, providing probe pulses in the visible spectral range from 480 nm to 760 nm. The pump pulses were generated by sum frequency mixing the fundamental amplifier output with visible pulses centered at 595 nm derived from a NOPA (non-collinear optical parametric amplifier)[34] in a BBO crystal. The resulting 2.5 uJ pump pulses were centered at 343nm with 8 nm bandwidth FWHM. The

pump fluence at the sample position was set to 0.3 mJ/cm^2 and the instrument response function was determined to be 130 ± 20 fs across the probe spectral range. The polarization of the pump and probe were set with respect to the crystals' orientation in order to maximize the visible absorption of the closed-ring isomer. Where specified, 270 nm pump pulses – generated by frequency tripling the fundamental – were used rather than 343 nm. Here the pump pulses impinge on a variable delay stage such that the path length of the pump is systematically varied relative to the probe in order to measure the temporal dependence of the pump induced change in optical density.

To ensure the same initial conditions for each pump-probe event, a continuous wave (cw) HeNe laser (λ = 633 nm) is used to convert all the molecules back to their initial open-ring state following each UV pump pulse. This is in contrast to conventional pump-probe spectroscopy which uses thermal reversibility or the constant exchange of sample (flow or translation) to ensure the same initial conditions. In addition to measuring the pump-on (I_{ON} (τ)) and pump-off (I_{OFF}) probe intensities necessary for the differential measurement, the "after" intensity (I_{ON}(2 ms)) is also measured to determine the degree of cyclization induced by the pump as reflected by the absorption profile of the now closed-ring molecules. To accomplish this, both the femtosecond UV pump and cw HeNe laser are controlled with individual shutters that are externally triggered. The pulse and acquisition sequence is the following: the spectrometer is set to acquire 7 consecutive probe pulses while the UV pump shutter is externally triggered to let only a single pulse hit the sample. This pump pulse is triggered to arrive only during the 6th probe pulse. The 7th probe pulse is acquired to determine the differential absorption associated with a time delay of infinity (τ_∞). Shortly after those 7 pulses, the shutter associated with the HeNe laser is opened for 500 ms to convert the closed-ring isomers to their initial state. This completes a single cycle, allowing the time delay (τ) to be altered and subsequent pump-probe events to be recorded. The time-dependent differential spectrum ($\Delta OD(\tau) = -\log_{10}(I_{ON}(\tau)/I_{OFF})$) is obtained by comparing the $I_{ON}(\tau)$ (6th) and I_{OFF} (average of the first 5) acquired probe spectra for each individual time delay. The τ_∞ spectrum ($\Delta OD(\tau_\infty) = -\log_{10}(I_{ON}(\tau_\infty)/I_{OFF})$) is obtained by comparing the "after" (7th) and pump-off probe intensities. Here τ_∞ is measured at approximately 2 ms after the pump pulse (i.e. I_{ON}(2 ms) = $I_{ON}(\tau_\infty)$) as determined by the 500 Hz repetition rate of the regenerative amplifier. It should be noted that 2 ms is an appropriate approximation of τ_∞ as no spectral evolution is observed from approximately 20 ps (*vide infra*) until exposure to visible light.

Averaging 5 pulses to determine I_{OFF} was chosen as a compromise between increased S/N due to averaging against the loss of correlation between the I_{ON}, I_{OFF}, and $I_{ON}(\tau_\infty)$ for the white light probe. Furthermore, only one pulse was consider for $I_{ON}(\tau_\infty)$, as the white light probe pulses were found to convert a small but measurable portion of the molecules to their initial open form. As such, the magnitude of the τ_∞ signal was systematically lower (by approximately 2-3 %) by considering, for example, the 11th rather than the 7th probe pulse. Furthermore, it should be noted that the duty cycle of this acquisition method is limited by the use of 500 ms of cw-HeNe exposure to ensure full cycloreversion. Due to the sequential two-photon nature of the cycloreversion process[18,23,24,26-29] the use of picosecond pulses to revert the system at each excitation event,

rather than cw visible excitation, could in principle increase the duty cycle. However, the general approach associated with externally triggered shutters is necessary when dealing with samples of limited reversibility so that the pump pulse is not continuously impinging on the sample.

The time resolved electron diffraction measurements were conducted in parallel using a newly developed 100 KV electron gun that is a modified version of previous work[35], with improvements in the magnetic lenses and beam transport. In time-resolved electron diffraction, a femtosecond laser pulse excites the sample under study and an ultrashort photoelectron bunch probes its structure via diffraction; by varying the time delay between the laser and electron pulses, the recorded diffraction patterns temporally resolve the structural changes. For the present study, 270 nm pump pulses were used and the photoelectron bunches contained approximately 5 x 10^5 electrons/pulse. Similarly to the optical measurements, a cw HeNe laser was irradiated on the sample between each pump-probe event to convert all the molecules back to their initial open ring form.

Powdered 1,2-bis(2,4-dimethyl-5-phenyl-3-thienyl) perfluorocyclopentene was purchased from Tokyo Chemical industrial Co. and dissolved in hexane (5g/L). The single crystals were grown in the dark by slow solvent evaporation from a flat bottom beaker container. Flat crystals with area on the order 0.1 to 1 mm^2 and thickness on the order of 100 um were selected for the experiment. Single-crystallinity was confirmed by electron diffraction. For the optical measurements, the crystals were mounted on top of a metallic 100 um pinhole used to ease the alignment. For the electron diffraction measurements, the crystals were microtomed to 100 nm and mounted on standard TEM copper grids. The linear absorption measurements were performed on a Cary UV-Vis spectrometer with linear polarizers.

Geometries of the open and closed ring isomers were optimized at the B3LYP/6-31G(d) level of theory using the default Berny optimization algorithm as implemented in the GAUSSIAN09 software package[36]. For minimum-energy structures obtained from the density functional theory DFT calculations, vibrational frequency calculations were performed, and electronic excitation spectra were calculated using the time-dependent density functional theory (TDDFT) formalism[37].

3. Results and discussion

3.1 Steady state absorption spectra

Figure 1 shows the linear absorption spectra for the open- and closed-ring isomers of the diarylethene derivative seen in Scheme 1. These spectra are taken for two orthogonal polarizations of light which exhibit maximum and minimum absorption in the visible for the closed-ring isomer. A cw UV-lamp with broad band emission was used to induce the ring-closing of the molecules in the initially open-ring crystal. A cw HeNe laser (λ = 633 nm) could then be used to convert the molecules back to the open-ring form. The measured

spectrum for the polarization with maximum absorption is similar to that previously reported for this compound[38].

The open-ring form is essentially transparent in the visible region with the observed offset of approximately 0.2 being due to reflections on the front and back crystal surfaces as well as reduced transmission due to surface roughness and scatter. In contrast, the closed-ring form exhibits a broad absorption band in the visible. The feature is centered around 635 nm and as a FWHM of approximately 150 nm. Furthermore, the absorption spectra of the closed-ring form exhibits a strong anisotropy. This was also observed in many other crystalline diarylethene derivatives[5,39] and is expected for the crystalline phase due to the orientation of the molecules and their associated transition moments. For the time-resolved measurements presented in section 3.3, the polarizations of both the pump and probe were parallel and oriented along the direction of maximum absorption in the visible for the closed ring form.

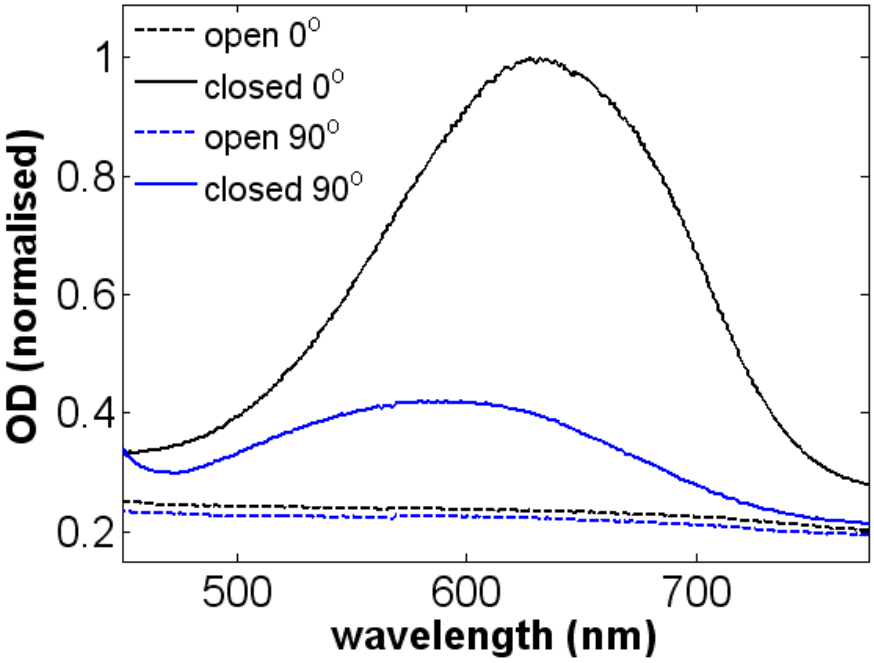

Figure 1. Linear absorption spectra for the open- and closed-ring isomers of the crystalline diarylethene derivative used. These spectra are for two orthogonal orientations of light linearly polarized along the directions exhibiting maximum (0º) and minimum (90º) absorption in the visible (in the closed-ring form). Cyclization (open → closed) is induced by irradiation with cw UV and cycloreversion (closed → open) is induced by irradiation with a cw HeNe at 633 nm (see Scheme 1).

3.2 Cycling repeatability

As previously discussed, the ability to apply the technique of transient differential absorption to the cyclization reaction of interest requires that the individual pump-probe events experience the same initial conditions. To achieve this in the single crystal phase, without translation of the sample, complete cycloreversion to the transparent open-ring isomer must be ensured prior to the arrival of every UV pump pulse. If the cycloreversion was incomplete the probe transmission would experience an overall decay due to the accumulation of the closed-ring compound and absorptions associated with the closed-ring isomer would begin to contribute to the transient signal. Complete cycloreversion is easily satisfied by prolonged exposure to a cw HeNe laser following every UV pump pulse. In addition, for the time-resolved experiment the limited fatigue resistance of the sample must be investigated for the pump conditions used.

Diarylethene crystals (including1,2-bis(2,4-dimethyl-5-phenyl-3-thienyl) perfluorocyclopentene) have been reported to undergo more than 10^4 cw-induced ring-opening and ring-closing cycles before significant reduction in the photochromic properties were observed[5]. Due to the thermal stability of the closed-ring isomer, the pump induced change in optical density well after the ring-closing reaction has occurred, $\Delta OD(\tau_\infty)$, is a direct measure of this optical fatigue. As the photochromic properties of the system are compromised, the magnitude of $\Delta OD(\tau_\infty)$ will decrease. In order to ensure that undesirable side products associated with this reduction in photochromicity[1,40,41] do not contribute to the transient signal, the pump induced change in the optical density can be measured at 2 ms – effectively τ_∞ – after every pump pulse as described in section II. This acquisition method ensures that the sample is in the requisite fully reversible and undamaged regime.

Figure 2(a) presents the optical fatigue measurements for a single crystal diarylethene derivative pumped by successive single pulses of 343 nm with a fluence of 0.3 mJ/cm^2. Between individual cycles 500 ms of HeNe is used to ensure complete cycloreversion. The average $\Delta OD(\tau_\infty)$ spectra for cycle numbers 1-1000, 50001-51000, and 100001 - 101000, are presented. As is apparent, and expected from the previous reports of optical fatigue, the magnitude of the spectra are progressively decreasing as the number of cycles are increased. The inset of Figure 2(a) presents the $\Delta OD(\tau_\infty)$ at the center of the closed-ring absorption band (635 nm) as a function of the cycle number. Within the fluctuations of pump fluence, the magnitude of the first 3 x 10^4 cycles is essentially constant. However, after this point a clear downward trend is observed. Such "two-phase" behavior is consistent to that previously reported in a similar diarylethene derivative in the crystalline phase[42]. Figure 2(b) presents similar measurements for a pump wavelength of 270 nm with equal number of photons in each excitation pulse (0.4 mJ/cm^2). The average $\Delta OD(\tau_\infty)$ spectra for cycles 1-200, 401-600, and 2401-2600, are presented. Once again the inset of Figure 2(b) presents the $\Delta OD(\tau_\infty)$ at the center of the closed-ring absorption band (635 nm) as a function of the cycle number. The optical fatigue following pulsed excitation with 270 nm is observed to be approximately 2 orders of magnitude faster than observed with excitation at 343 nm.

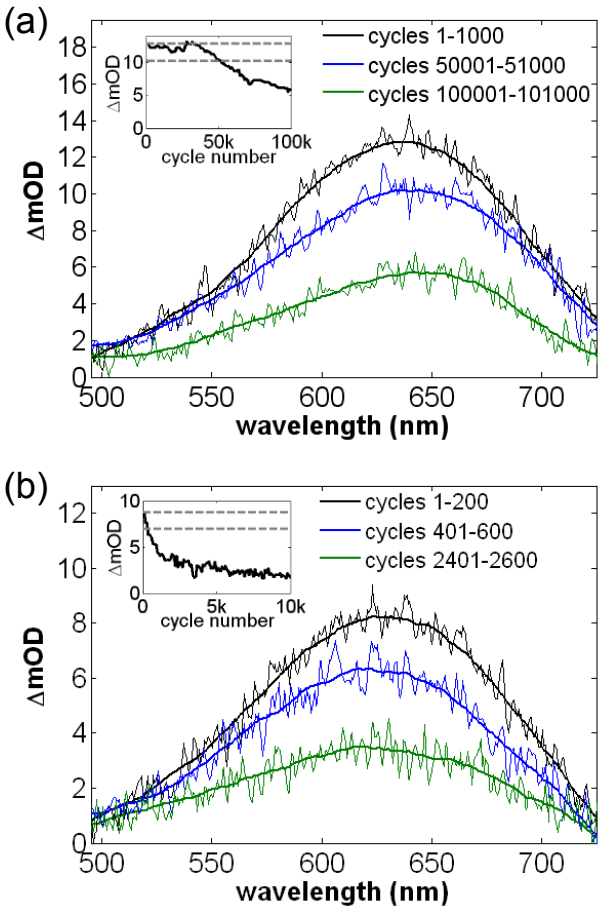

Figure 2. (a) Average $\Delta OD(\tau_\infty)$ (taken 2ms after the pump) induced by single pulses of 343 nm (100 fs, fluence = 0.3 mJ/cm^2) for cycles number 1-1001, 50001-51000, and 100001-101000. (b) Average $\Delta OD(\tau_\infty)$ spectra induced by single pulses of 270 nm (100 fs, fluence = 0.4 mJ/cm^2) for cycles number 1-200, 401-600, and 2401-2600. The insets show the $\Delta OD(\tau_\infty)$ at 635nm as a function of the cycle number, with the dotted lines representing the 100% and 80% levels.

Based on extinction coefficients from solution phase measurements and qualitative evaluation of the transmission in thin crystals, the penetration depth of 270 nm pump is dramatically shorter than that of 343 nm[43]. Though estimates from solution phase data are relatively coarse as the crystalline environment is known to influence the absorption spectrum[44], the general order of magnitude suggests that the photoexcited molecules are localized much nearer the surface of the crystal when using 270 nm excitation. This implies that the concentration of excited states under these conditions is significantly higher in the surface region, possibly leading to faster optical fatigue. Furthermore, the optical fatigue of diarylethene derivatives is known to be negatively influenced by the presence of oxygen[1,40,41], and we would anticipate that significant amounts of oxygen would permeate the first molecular layers of crystal relative to the bulk crystal sampled by 343 nm excitation. Alternatively, or in combination with the above suggestions, excitation with the 270 nm pump may

be capable of accessing higher energy excited states that possess additional reaction pathways towards undesirable side products. Regardless of the mechanism that limits the optical fatigue following 270 nm excitation to 100s of cycles, it is clear from Figure 2 that excitation with 343 nm allows for 3 x 10^4 cycles in the fully reversible regime. This wavelength dependence was important to establish as our initial efforts focused on the use of 270 nm pump pulses that are experimentally much easier to generate.

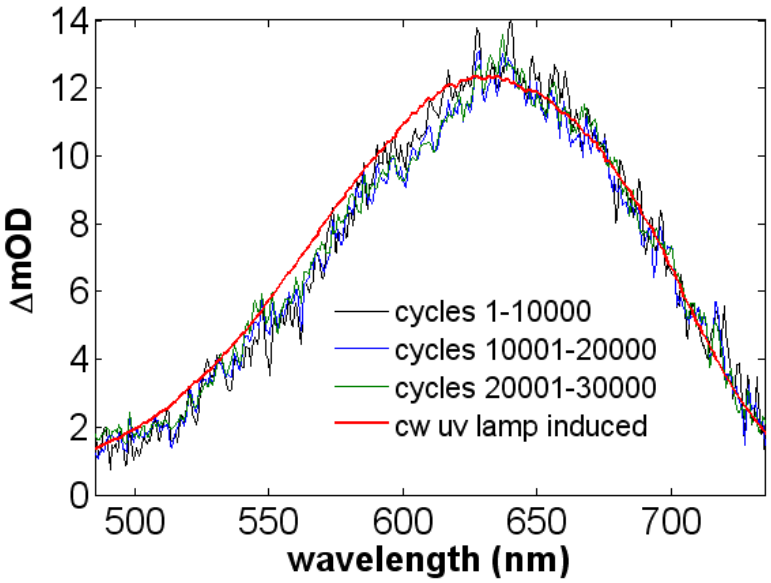

Figure 3. The average $\Delta OD(\tau_\infty)$ for the first 3 x 10^4 cycles (taken 2ms after the pumps) binned in 1 x 10^4 cycles (blue, green, and black curves), following excitation with 0.3 mJ/cm^2 of a 343nm pump pulse. The red curve is the linear absorption spectrum for the closed ring compound presented in Figure 1, after offset correction and rescaling to match the magnitude reached with the fs pump excitation. The convergence of the first 3 x 10^4 cycles is apparent.

Figure 3 presents the first 3 x 10^4 cycles of the measurement presented in Figure 2(a), averaged in groups of 1 x 10^4 cycles. The first 3 x 10^4 cycles are essentially identical. Figure 3 also shows for comparison the linear absorption spectrum for the closed-ring compound induced with a cw UV lamp, which was presented in Figure 1. After offset correction and rescaling to match the magnitude reached with pulsed excitation, it is apparent that the pump induced changes in optical density at infinite time delays converge to the linear absorption spectrum of the closed-ring compound. The small discrepancy is due to the very high sensitivity of the absorption spectrum to the relative orientation between the crystal and the polarization of the probe light. Figure 3 confirms that, for the first 3 x 10^4 cycles, the sample is indeed fully reversible and undamaged. As such, only these cycles were used for extracting the transient dynamics presented below.

3.3 Transient absorption measurements

In the previous section (section 3.2) it was established that pulsed excitation at 343 nm allowed the diarylethene derivative to undergo 3 x 10^4 successive ring-closing and ring-opening cycles before the onset of optical fatigue. As such, the pump-probe measurements extracted from this range of cycles adhere to the requisite criteria of reversible reaction conditions. However, it should be emphasized that this limitation in the reversibility would correspond to approximately 1 minute of acquisition for a conventional pump-probe measurement (1 kHz system). Here the transient dynamics are recoverable due to the pulse sequence outlined in section II.

The transient differential absorption measurements corresponding of the ring-closing reaction in the single crystalline diarylethene derivative are displayed in Figure 4. These measurements correspond to the first 3 x 10^4 cycles and are a result of excitation at 343nm with a fluence of 0.3 mJ/cm^2. To provide an overview of the ring-closing dynamics, the contour plot of the temporally resolved transient differential absorption spectrum is presented in Figure 4(a). Selected spectra for various time delays between -200 fs and 50 ps, compared to their associated τ_∞ measurements, are presented in Figure 4(b). The data were corrected for white-light chirp. It is important to emphasize that the amplitude of the τ_∞ spectra were not rescaled to that of the transients; they are the measured spectra at 2 ms after the pump pulses, taken together with every transient measurement (section II). The formation of the spectra associated with the closed ring molecules is clearly observed. After approximately 20 ps, the transient spectrum is essentially fully converged to that of the final product, where it remains static until the application of visible light is used to induce the cycloreversion process.

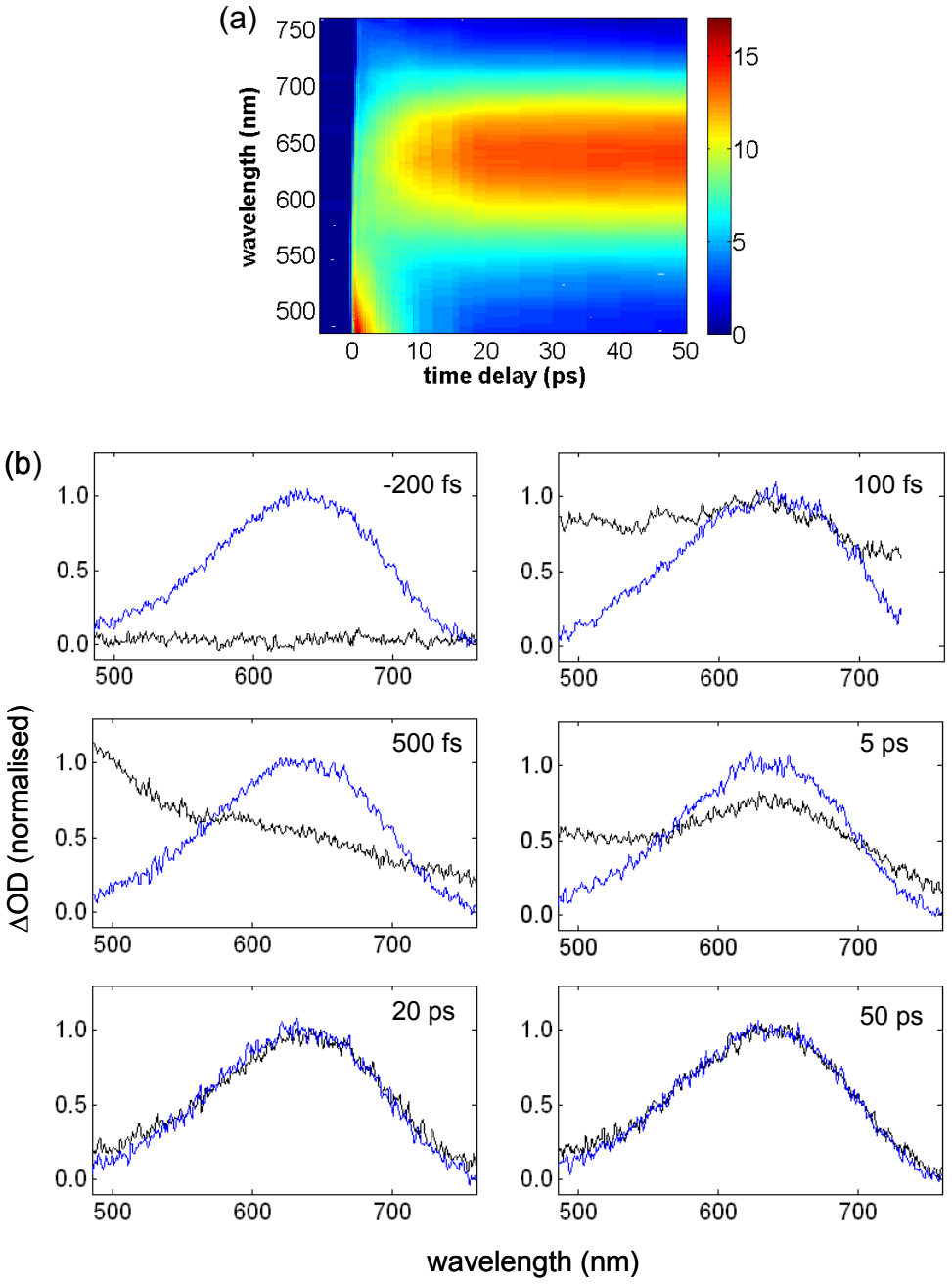

Figure 4. Transient absorption measurements of the ring-closing reaction in the single crystalline diarylethene derivative by pumping at 343nm (fluence = 0.3 mJ/cm^2). (a) Contour plot of the transient absorption spectra as a function of time delay. (b) Selected spectra for various time delays between -200 fs and 50 ps (black curves), compared to their associated τ_∞ measurements (blue curves). The 100 fs spectrum was extracted from a separated dataset taken with higher resolution time steps.

As can be seen in the transient spectrum of Figure 4(b) corresponding to a delay of 100 fs following excitation, there is a broad initial absorption feature which extends across the entire detection range. In the

frame corresponding to a delay of 500 fs, the absorption maximum is seen to have rapidly shifted towards the blue. Following this sub-ps evolution, the blue feature decays on the 5 ps time scale along with the simultaneous formation of a feature which exactly corresponds to the closed-ring absorption spectrum. It is apparent from Figure 4 that there are relevant dynamics on both the femtosecond and picosecond time scales. As will be elaborated below, the dynamics on the femtosecond time scale are associated with the structural relaxation within the excited state of the open-ring isomer, while the dynamics on the picosecond time scale are associated with the actual ring-closing reaction.

3.3.1 Femtosecond dynamics

The presence of dynamics on the femtosecond time scale is apparent in Figure 4 of the previous section. The sub-picosecond dynamics following excitation with a 0.3 mJ/cm^2, 343 nm pump pulse are presented in greater detail in Figure 5, where the transient absorption spectra for time delays between 75 fs and 450 fs are depicted in Figure 5(a). The initially broad photoinduced absorption seen at 75 fs progressively shifts from the red (625 nm) to the blue (sub-480 nm) end of the visible spectrum in the first 500 fs following UV excitation. This spectral shifting is made more apparent in Figure 5(b) where, following Hania *et al.*[16], the individual wavelengths of the temporally resolved transient absorption spectrum are normalized to their maximum values in the sub-ps region. Here the progressive spectral shift is clearly exposed and is seen to occur on a time scale of a few hundred femtoseconds.

The normalized single wavelength transients centered at 485 nm, 600 nm, and 675 nm are extracted from Figure 5(b) and depicted in Figure 5(c). Bi-exponential fits with constant offsets (to account for the absorption profile of the thermally stable photoproduct) are convolved with the instrument response function and shown as solid lines. The second exponential is a relatively long time-constant of 5-7 ps, and was imposed to account for the subsequent picosecond time scale dynamics (see section 3.3.2). The resulting sub-ps time constants range from 100 fs to 290 fs and are shown in the individual frames.

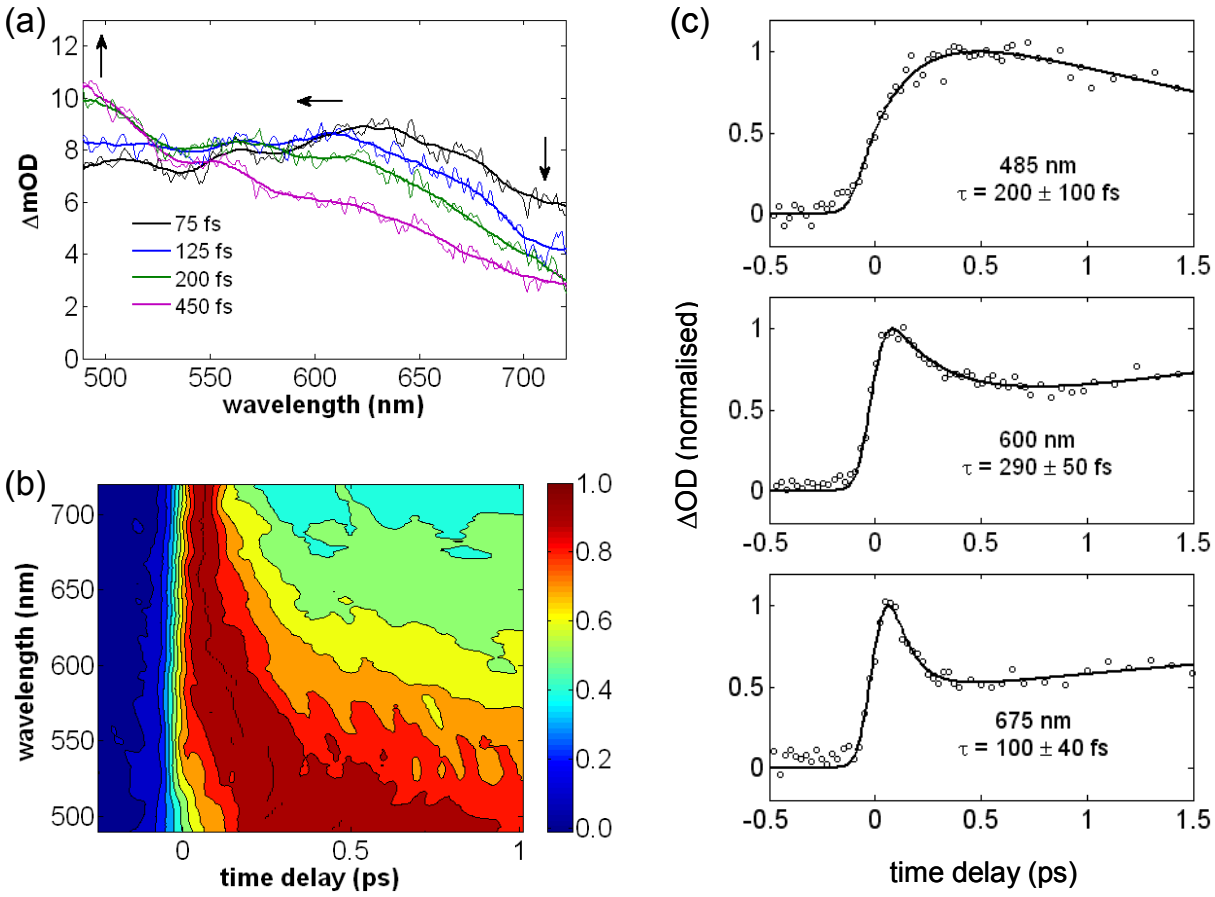

Figure 5. Femtosecond dynamics: evolution on the excited state potential energy surface of the open-ring isomer. **(a)** Transient absorption spectra for time delays between 75 fs and 450 fs. **(b)** The temporally resolved transient absorption spectrum where each wavelength is normalized to its maximum signal in the sub-ps region. **(c)** Single wavelength transients extracted from (b) at probe wavelengths 485 nm, 600 nm, and 675 nm. The solid lines represent bi-exponential fits where a long time-constant of 6 ps was imposed. The resulting sub-ps time constants are shown in the individual frames.

The transient in the red end of the spectral window, associated with 675 nm, has an initial instrument response function limited rise (or near instrument response function limited), and then decays rapidly (τ = 100 fs) to approximately 40% of its initial magnitude. The signal then experiences a secondary rise on the picosecond timescale associated with convergence towards its closed-ring magnitude (see section 3.3.2). This rapid decay indicates that the spectral shifting begins immediately following photoexcitation. The transient at 600 nm has a similar behavior as that of 675 nm, but with a slower decay (τ = 290 fs). Conversely, the transient centered at 485 nm exhibits a slow rise (τ = 200 fs) such that it does not reach its maximum value until approximately

500 fs. It then begins to decay towards its closed-ring magnitude on the picosecond timescale. It should be noted that the spectral characteristics associated with the transient absorptions seen in Figure 5(a) do not resemble the absorption profiles expected from the closed-ring isomer. Rather, this progressive spectral shift occurs prior to the ring-closure itself, and is attributed to the evolution on the excited state potential of the open-ring isomer due to the difference in the equilibrium geometry between the ground and excited states.

The photoinduced absorption band, whose maximum is initially at 635nm, is assigned to the excited state absorption of the open-ring molecules initially in the equilibrium geometry associated with the ground state charge distribution. As the Frank-Condon wave packet is driven towards the open-ring excited state potential energy minimum, the excited state absorption is seen to progressively blue shift, reflecting the increase in energy difference between the vibrationally relaxed excited state populations and higher lying electronic levels. The resulting absorption feature in the blue end of the probe's spectral range is therefore associated with the relaxed structure of the open-ring form in its excited state. The formation of this intermediate occurs with a time constant of 200 fs.

In contrast to the assertion that the sub-picosecond dynamics result from vibrational relaxation on the excited state potential of the open ring isomer, it should be noted that the timescale of this spectral shifting is also consistent with a polarization response of the surrounding crystalline lattice. In this case, the pump-induced electronic excitation on the molecular unit would result in reorientation of the surrounding polarizations in response to the change in charge density. However, the large magnitude of the spectral shifting observed in Figure 5(b) (more than 100 nm) is inconsistent with this intermolecular mechanism. Furthermore, projections of the ground state equilibrium geometry on the excited state potential are expected to occur well away from local minima in regions of relatively large curvature[33], which further supports the assignment that the large spectral shifting results from vibrational relaxation along the excited state surface as opposed to a polarization response of the surrounding medium (unexcited diarylethene molecules).

The sub-ps dynamics presented above are in qualitative agreement with previously reported results for similar diarylethene derivatives in solution. In particular, spectral shifting of the excited state absorption of the open-ring isomer, prior to the ring-closing reaction, was observed by Hania. *et al*.[13,16]. They also interpreted this shifting as a result of the relaxation of the open-ring isomer on the excited state potential energy surface, and supported this interpretation by semiempirical calculations of the ground and excited state potential energy curves along the reaction coordinate. In addition, several other solution phase studies have also identified the formation of this intermediate for related compounds on sub-ps time scales[7,11,12]. However, the work presented here represents the first measurement done with sufficient temporal resolution to resolve its formation in the crystalline phase. The vibrational analysis provided in section 3.6 will further discuss the specific atomic motions involved in the formation of this reaction intermediate.

3.3.2 Picosecond dynamics

Figure 6(a) shows the convergence on the picosecond time scale of the transient differential absorption towards that of the closed-ring photoproduct. Here, selected transient spectra for time delays between 0.5 ps and 50 ps are displayed. Once again, the transient signals are seen to converge to the expected absorption profile of the closed-ring photoproduct within 20 ps. There are two distinct contributions to the transient absorption signals presented in Figure 6(a). Initially the excited state absorption associated with the open-ring isomer (see section 3.3.1) dominates the signal on the sub-ps timescale. Following relaxation in the excited state potential of the open-ring structure, the spectral feature associated with this intermediate, seen in the blue end of the detection range, decays in concert with the growth of the ground state absorption associated to the closed-ring isomer centered at 635 nm.

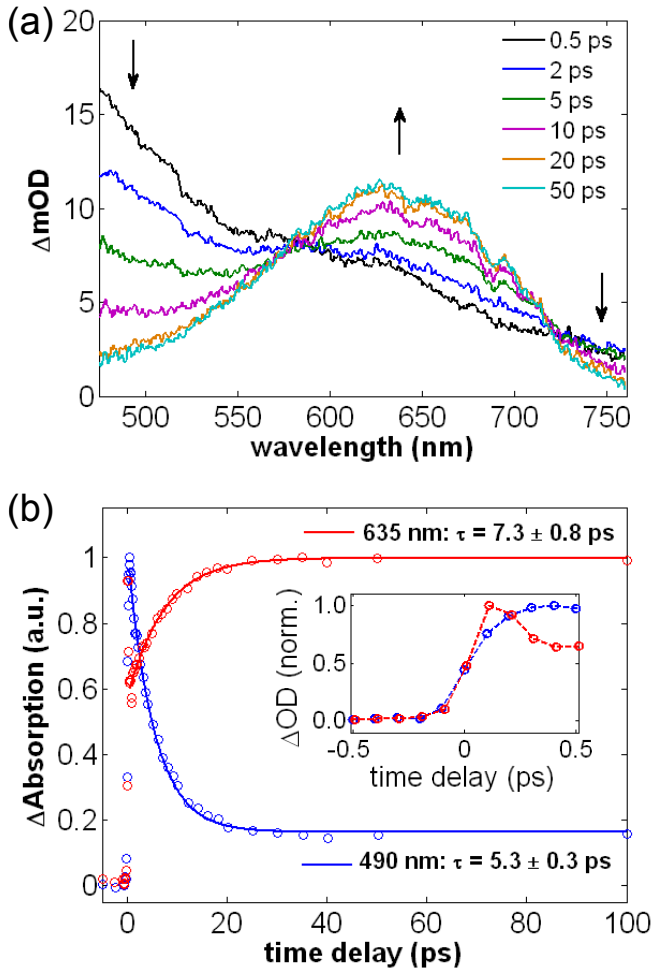

← ***Figure 6.*** 3 x 10^4 cycles were used for this dataset. The pump was centered to 343 nm, with a fluence of 0.3 mJ/cm^2. (a) Transient absorption spectra for time delays between 0.5 to 50 ps. (b) Transient traces for the probe wavelengths 635 and 490 nm. Mono-exponential fits (with constant offsets to account for the closed-ring system) are shown, with time constants of 7.3 and 5.3 ps for 635 nm and 490 nm, respectively. The fits consider only the time points after 0.5 ps in order to exclude the more complicated femtosecond dynamics discussed in section 3.3.1. The inset demonstrates the sub-ps behavior.

Figure 6(b) shows the transient time traces for the probe wavelengths at 635 nm and 490 nm. The former is the central wavelength of the absorption feature associated with the ground state absorption of the closed-ring

isomer and follows the growth of the photoproduct. The latter follows the decay of the excited state absorption associated with the relaxed open-ring structure. Mono-exponential fits with constant offsets are shown as the solid lines. The time constants, τ, for the rise and decay of the signals at 635nm and 490 nm are 7.3 ± 0.8 ps and 5.3 ± 0.3 ps, respectively.

It was anticipated that the rise and decay of the signals seen in Figure 6(b) would be equally matched, as the closed-ring photoproduct is thought to be directly formed from the relaxed excited state of the open-ring structure through a conical intersection[33]. However, following the radiationless transition from the excited state of the open-ring to the ground state of the closed-ring, there is an expected excess of vibrational energy and the discrepancy in the time constants can be largely attributed to the vibrational relaxation of the nascent photoproduct[18]. That is, the growth of signal at 635 nm on the picosecond timescale is convolved with the cyclization reaction, vibrational cooling, and lattice relaxation to give the spectra corresponding to the ground state closed-ring form. In addition, the transient associated with 635 nm is complicated by the broadness of the excited state absorption associated with the open-ring isomer. As can be clearly seen in Figure 5 of section 3.3.1 and in the transient spectrum at 0.5 ps in Figure 6(a)**,** this initial photoinduced absorption is non-zero across the entire visible region. As such, it is less ambiguous to consider the decay of the relaxed excited state absorption associated with the open- ring structure to assign the time constant of the ring-closing reaction, which we conclude to occur with τ = 5.3 ± 0.3 ps.

The time constant of 5.3 ± 0.3 ps obtained for the ring-closing reaction is in qualitative agreement with previous studies of similar diarylethene derivatives in the crystalline phase[8,18]. However, the time resolution of these previous studies was limited by the use of a 15 ps pump pulse. To our knowledge this is the first measurement that fully resolves the cyclization reaction of a diarylethene derivative, from the initial motion on the excited state surface to full ring closing, in the crystalline phase. It is also the first measurement based entirely on the photoreversibility of the reaction to provide well defined reference spectra, making it possible to do the measurements on small, but high quality, portions of the photochromic single crystals.

The simplicity of the dynamics observed is Figure 6 differs markedly from most of the previously reported results on similar diarylethene derivatives in solution[7,10-13,16]. In particular, the formation of the ring-closed molecule is unambiguous. By 20 ps, the transient spectrum is almost fully converged – both in shape and in amplitude – to that of the final photoproduct. In solution, discrepancies between the transient spectra and that of the final closed-ring product are generally observed at relatively late time delays due to a racemic mixture of the open-ring isomer. Specifically, the parallel (C_S symmetry) enantiomer is unable to undergo cyclization, while the antiparallel (C_2 symmetry) structure (seen in Scheme 1) is believed to do so with unity quantum yield for a large number of diarylethene derivatives[1,45]. Thus, in a racemic mixture, the quantum yield for cyclization of such derivatives is approximately 0.5[5,43]. Though the parallel structure does not contribute to the cyclization reaction, it has been found to have long-lived excited states absorption bands that interfere with the ability to clearly resolve the spectral feature associated with nascent ring-closed molecules[7,11-13,16]. Conversely,

single crystal diarylethene derivatives are generally composed exclusively of the antiparallel arrangement, resulting in essentially unit quantum yields[5,38]. In the crystalline phase, the periodic structure enables all the excited molecules to undergo cyclization under nearly identical local environments. This high level of uniformity in local environment and conformation imposed by the crystal structure leads to the unique transient absorption signal, which maps out the pathway to the ring-closed linear absorption spectrum.

Previous studies which employed femtosecond temporal resolution in the solution phase have obtained time constants associated with cyclization ranging from sub-ps to sub-3 ps for similar fluorinated diarylethene derivatives with heterocyclic aryl groups[7,9,10,14,16]. Here, the cyclization reaction in the crystalline phase is found to be significantly slower, presumably due to the impeding influence of the close-packed environment. A similar observation and interpretation was reported for the cycloreversion reaction in a crystalline diarylethene derivative[27]. The fact that the photochromicity of 1,2-bis(2,4-diethyl-5-phenyl-3-thienyl) perfluorocyclopentene is preserved in the crystalline phase suggests that the structural changes necessary for cyclization are relatively small when compared to other photochromic molecules[5]. Despite this, the intramolecular motions are still significant, and presumably highly constrained, in the context of the close-packed conditions associated with the single crystal phase. The impeding influence of the crystalline environment on the cyclization reaction has been explicitly demonstrated in an X-ray crystallographic study which showed that the structure of the closed-ring molecules inside a crystal of the initially open-ring form was distorted[44]. This observation, in tandem with the increased timescale for the cyclization in the crystalline phase, implies that the intermolecular contacts associated with the periodic crystal structure hinder the nuclear motions necessary for the cyclization reaction.

3.4 Signature of optical fatigue in transient signals

As a final note we briefly explore the transient spectral features associated with optical fatigue of a photochromic diarylethene derivative in the crystalline state. In section 3.2 it was established that the diarylethene derivative of interest possessed 3 x 10^4 cycles before the onset of damage. However, as was apparent in Figure 2(a) of section 3.2, the optically fatigued crystal still continued to display photochromicity of reduced magnitude even after 1 x 10^5 cycles. In order to demonstrate the influence of the fatigued sample on the transient dynamics, Figure 7(a) presents the transient absorption spectra 5 ps following excitation with 0.3 mJ/cm^2 of 343 nm pulsed light for the entire 1 x 10^5 cycles investigated. The spectra presented are normalized to their respective τ_∞ (2ms) signals and binned in groups of 2 x 10^4or 4 x 10^4 as specified.

It can be observed that there is already a small discrepancy between the transient measurement corresponding the first and second 2 x 10^4 cycles. As the number of cycles increase, the sample becomes progressively more fatigued and the discrepancy dramatically increases. Though the crystal may still display photochromic properties of reduced magnitude (see Figure 2(a) of section 3.2), it is not possible to simply scale the transient

data to the τ_∞ magnitude to compensate for this reduction. This is because the optical fatigue is due to the formation and accumulation of undesired photoproducts[1,40,41] which also display transient dynamics in the same spectral region as those associated with the cyclization reaction. To demonstrate this point, Figure 7(b) presents the transient absorption spectra of the fatigued diarylethene derivative. The spectra are extracted from cycles 6 x 10^4 to 1 x 10^5 for time-delays between 0.5 and 50 ps. In contrast to the unfatigued cyclization reaction extracted from the first 3 x 10^4 cycles, the transient spectra no longer converge to the τ_∞ spectrum, even at 50 ps. Apparently, long lived photoinduced absorptions unrelated to the cyclization reaction distort the dynamics of interest.

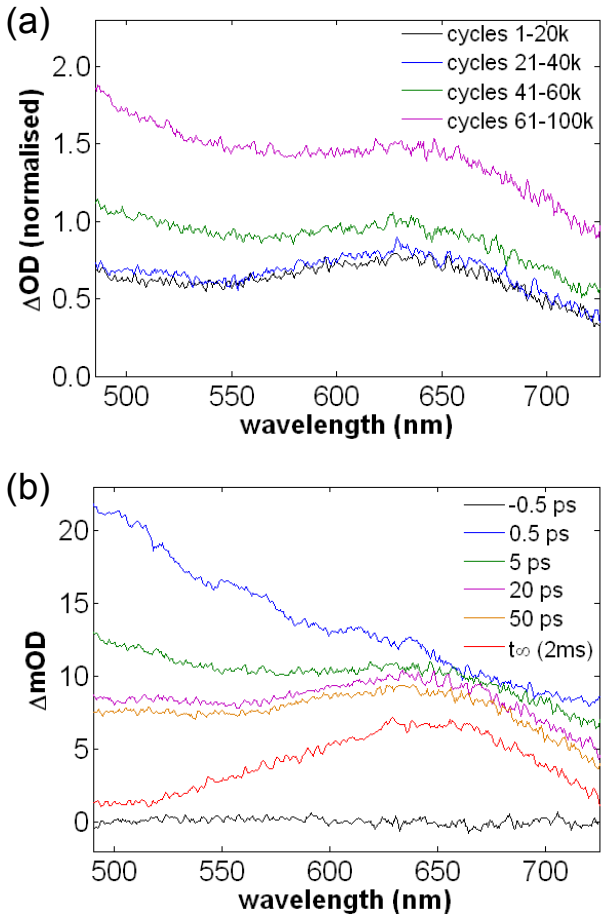

← ***Figure 7.*** (a) Transient absorption spectra 5 ps following excitation with 0.3 mJ/cm^2 of 343 nm pulsed light for the entire 1 x 10^5 cycles investigated. The spectra presented are normalized to their respective τ_∞ (2ms) signals and binned in groups of 2 x 10^4or 4 x 10^4 as specified. (b) Transient absorption spectra for time-delays between 0.5 and 50 ps from an optically fatigued, single crystal diarylethene derivative. These dynamics are extracted from cycles 6 x 10^4 to 1 x 10^5.

3.5 Electron diffraction studies: direct observation of picosecond structural dynamics

The convergence of the transient spectra to the fully relaxed ground state of the closed ring isomer seen in section 3.3.2 provides direct evidence for assigning the observed dynamics to the cyclization reaction. However, it must be noted that the optical techniques employed in the previous section are only indirectly sensitive to the structural changes associated with the chemical reaction. The relationship between the implied atomic displacements and the observed ultrafast dynamics can be further demonstrated through the use of time-resolved electron diffraction, which is exquisitely sensitive to the structural changes.

Figure 8(a) shows the electron diffraction pattern of a 100 nm microtomed diarylethene single crystal in its initial open-ring state. Following UV irradiation, the diffraction pattern is expected to be altered as a result of the formation of ring-closed molecules within the open-ring crystal lattice. Furthermore, the changes are expected to be reversible by irradiation with visible light and repeatable for a large number of cycles. The dependence of the (7 -1 -6) diffraction peak on the photocycling process is depicted in Figure 8(b). Here the normalized diffraction intensity following subsequent illumination by single UV pulses (270 nm, 100 fs, 1 mJ/cm^2) and cw visible light (633 nm, 5 seconds, 2mW) is reported for 20 cycles. This result clearly confirms that the system is indeed structurally driven from the ring open to ring closed isomers, and further demonstrates that the structural change is photoreversible. Seeing the effect of the photocycling directly in terms of the structural changes to the crystal lattice provides additional evidence for both the photocycling and the robust nature that this process.

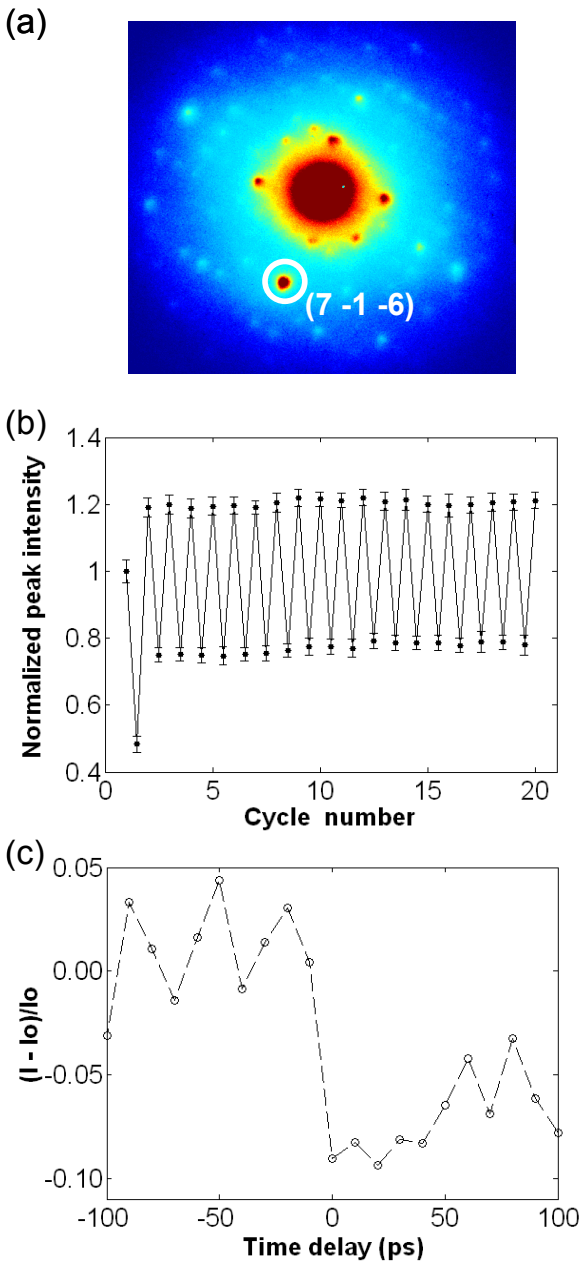

Figure 8. → (a) Electron diffraction pattern of the initially open-ring crystal. The diffraction peak (7 -1 -6) is circled. (b) Normalized integrated intensity of the diffraction peak (7 -1 -6) for the first 20 ring-closing and ring-opening cycles. (c) Time resolved change in intensity of the diffraction peak (7 -1 -6) associated to the ring-closing reaction. Adapted from reference [46].

Preliminary time-resolved diffraction results are presented in Figure 8(c) for the same diffraction peak. Although there is insufficient temporal resolution with respect to time steps to clearly resolve the initial motions along the reaction coordinate in this figure, the changes in diffraction intensity on the picosecond time scale are clearly evident, directly confirming atomic displacements on this time scale. This observation, in addition to the convergence of the transient spectra on picosecond timescales seen in section 3.3.2, provides incontrovertible evidence that the transient features are in fact related to the stated photochemical reaction dynamics and not other possible nonradiative relaxation processes.

Electron diffraction studies represent a very important advance in the study of chemical reaction dynamics. We have now successfully demonstrated both how to make and characterize molecular crystals for femtosecond electron (or X-ray) diffraction studies, as well as how to optically prepare a reaction coordinate under fully synchronized conditions to map out the primary motions involved. Though the proper interpretation and phasing of the diffraction data to project out the specific motions involved requires additional analysis, which is beyond the scope of this paper, the diffraction data does allows us to confirm that the noted transient absorptions are due to structural changes.

3.6 Theoretical considerations

Due to the potential applications of photochromic materials and their rather unusual properties, there has been a great deal of theoretical work done on diarylethene excited state dynamics[22,33,47-52]. The most notable work in this regard is that of Robb and coworkers, who have used complete active space (CASSCF) calculations and dynamics (molecular mechanics-valence bond, MMVB) on a hydrocarbon model system that is highly relevant to the present derivative under investigation in this report. Their work demonstrated that the mechanism of photochemical ring closing and ring opening reactions involves the system traversing through a conical intersection between the ground state S_0 and the first excited state S_1. The presence of additional conical intersections on the potential energy surface was also determined, which causes great difficulty when attempting to obtain optimised geometries on the S_1 surface. For example, time-dependent density functional theory (TD-DFT), which is the method of choice for a system of this size, is well known to fail to converge in the vicinity of a conical intersection. The way forward is to use a more rigorous approach to constructing the excited-state Slater determinants, such as that offered by the complete active space method. However, the high computational demands of this method invariably require that a simpler model system be constructed. In this regard we are therefore extremely fortunate that the work by Robb *et al* precedes us.

The results from our TD-DFT calculations on the full 1,2-bis(2,4-dimethyl-5-phenyl-3-thienyl) perfluorocyclopentene compound appear in Table 1. It is clear from our calculations that the $S_0 \rightarrow S_1$ excitation is mostly a one-electron HOMO $\rightarrow$ LUMO transfer, which are the bonding and antibonding orbitals between the two carbon atoms which join when the ring is fused. Their identities switch as we pass through

the conical intersection: for the closed-ring isomer the HOMO is the bonding orbital, whereas for the open-ring isomer the HOMO is the anti-bonding orbital. It can be seen in Table 1 that TD-DFT predicts that the first bright transition is $S_0 \rightarrow S_3$ at 4.3 eV for the open-ring form and $S_0 \rightarrow S_1$ at 2.1 eV for the closed-ring form, which is qualitatively consistent with the linear absorption spectrum[43] and the experimental observation that cyclization is induced by UV-light while the cycloreversion is triggered by visible light. It should be noted that the excitation conditions used to extract the transient dynamics seen in section 3.3 are near resonant with the weak $S_0 \rightarrow S_1$ transition of the open-ring isomer.

Prior work[33] suggests that the mechanism for closing the ring appears to be as follows. Photoexcitation to the S_1 surface, possibly following internal conversion from higher lying states such as S_3, will result in rapid relaxation from the Franck-Condon open-ring ground state geometry to a minimum on S_1. This initial relaxation involves large motion along the reaction coordinate defined as the distance between the two reactive carbon atoms, but is still clearly associated with the open-ring form. The large amount of kinetic energy resulting from formation of this initial intermediate is then redistributed among the numerous vibrational modes of the molecule. After some period of time, the conical intersection located in the vicinity of the S_1 open-ring minimum is reached through motions orthogonal to the reaction coordinate. Once this conical intersection is reached, the system then decays radiationlessly to S_0, followed by vibrational relaxation along the S_0 potential of the closed-ring form. The simulated dynamics propagated on the MMVB potential energy surface[33] suggests a two-timescale cyclization mechanism. The S_1 open-ring geometry forms rapidly, followed by the formation of a vibrationally hot closed-ring photoproduct, as limited by the ability of the S_1 open-ring intermediate to access the conical intersection through motions orthogonal to the reaction coordinate. This is precisely the behavior observed experimentally in section 3.3.

open-ring isomer			closed-ring isomer		
excitation energy (eV)	Oscillator strengths	major orbital change(s) contributing to the transition	excitation energy (eV)	Oscillator strengths	major orbital change(s) contributing to the transition
3.5568	0.0483	HOMO → LUMO	2.1113	0.2987	HOMO → LUMO
3.7761	0.0138	HOMO–1 → LUMO	3.0285	0.0223	HOMO–1 → LUMO
4.3319	0.3311	HOMO → LUMO+1	3.4783	0.1627	HOMO → LUMO+1
4.3336	0.0406	HOMO → LUMO+2	3.6857	0.0174	HOMO → LUMO+2
4.3642	0.1658	HOMO–2 → LUMO	3.9289	0.1308	HOMO–2 → LUMO HOMO → LUMO+3

Table 1. Excitation energies and oscillator strengths of the open- and closed-ring isomers for the five lowest excited states.

The key question that remains is the identity of the vibrational mode(s) that directs the motion along the seams of the conical intersection. Clearly, we must be looking for motion that modulates the carbon-carbon gap involved in the bond formation. Furthermore, given the requisite conrotary motion to establish the quasi-planar closed-ring structure, we anticipate the involvement of torsional motions of the pendant phenyl-thienyl groups. In the present work, we have extremely well defined dynamics thanks to the homogeneous intermolecular potential provided by the crystal lattice. The predicted initial motion of the ring closing process has been fully resolved and associated with a time constant of 200 fs. Presently, we are not able to invert the complementary time-resolved electron diffraction data to give the precise motions involved. This work is in progress and will be reported separately. We can, however, perform a modal analysis to see what motions are most likely involved in this initial displacement along the excited state surface.

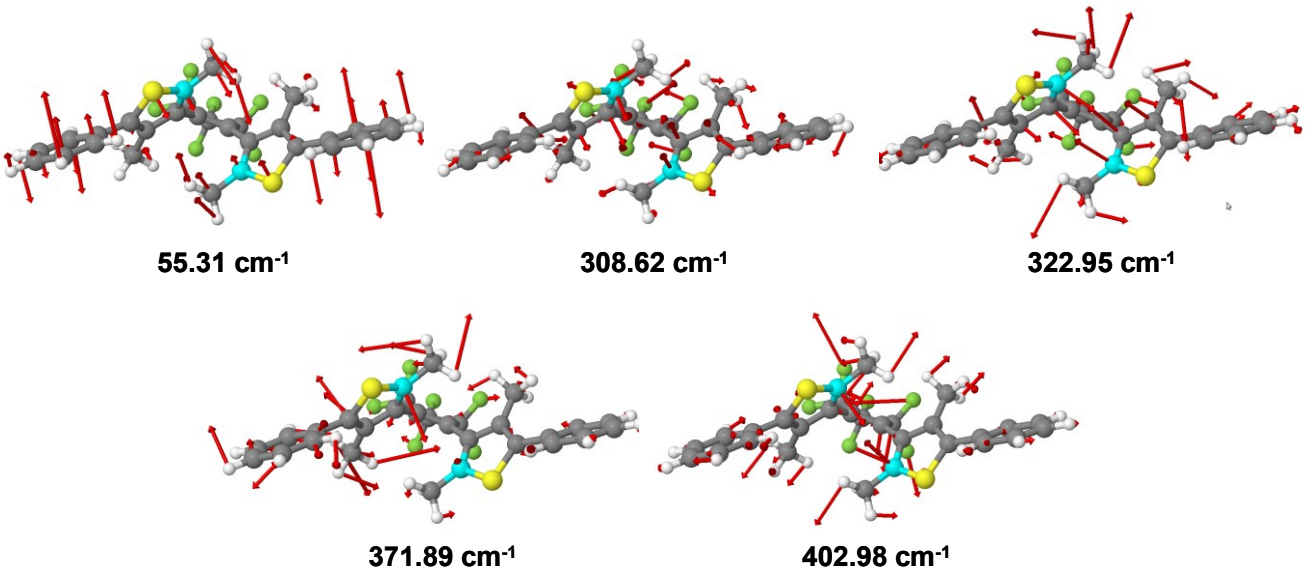

Figure 9. Low-frequency normal modes of the open-ring isomer which involve large changes in the C–C distance. The atomic displacement vectors are drawn as red arrows. The reactive carbon atoms are displayed in cyan.

The low-frequency normal modes of the open-ring isomer which involve large changes in the C–C distance are displayed in Figure 9. The lowest vibrational mode calculated for the ground state open-ring structure appears to match the atomic motion and timescale requirements. At 55 cm^{-1} it corresponds to a half-cycle of vibration of approximately 300 fs, and the eigenvector (see Figure 9) does indeed involve torsional motion of the two pendant groups to shorten the C-C gap. Of course, we must point out that this motion relates to the optimized structure on the S_0 surface, not S_1, upon which the reaction actually takes place. It was not possible to calculate excited-state vibrational frequencies as attempts to locate optimized geometries (either ring open

or closed) on the excited state surface using TD-DFT failed, probably due to the presence of nearby conical intersections. It is reasonable to expect some difference in the potential energy as a function of C-C distance for the S_0 and S_1 surfaces, which may result in perturbations to the vibrational modes. Additionally, it must be noted that the large displacements of the phenyl groups seen in the lowest frequency vibration of Figure 9 are likely to be heavily constrained in a single crystal lattice of the compound[3]. More generally, we anticipate that the initial sub-ps dissipation of excess energy on the S_1 potential of the open-ring form is accomplished through a superposition of the normal modes seen in Figure 9. The anharmonic coupling between these modes is evidently quite large to give the observed timescales, corresponding to nearly direct relaxation of the initial Franck-Condon modes to the lowest frequency modes involved in the initial motion along the reaction coordinate.

4. Conclusion

Transient differential absorption measurements were performed with femtosecond temporal resolution to investigate the cyclization reaction of a single crystal diarylethene derivative. These measurements clearly resolved the formation of a reaction intermediate on the 200 fs timescale which was associated with relaxation on the excited state potential of the open-ring isomer. Following this initial process, the cyclization reaction was clearly resolved and shown to occur with a time constant of 5.3 ps. These measurements were made possible by an acquisition scheme which exploited the photoreversibility and thermal stability of this specific crystalline system. Though this acquisition scheme is particularly valuable for photoinduced reactions that are thermally irreversible, it can be adapted to ensure the requisite reversibility for any time-resolved differential measurement where the constant exchange of sample is impractical. This aspect of the experimental methodology will also be of great utility for determining the peak power limitations for a time resolved diffraction experiment where the goal is to obtain the actual atomic motions related to the photoreaction of interest.

Though the timescale for the cyclization reaction is well established by this spectroscopic study, the precise nuclear motions associated with traversing the conical intersection associated with the isomerization remains unresolved. With improved analysis methods we expect to be able to report on the principle motions from the direct observations of the structural dynamics in reciprocal space using electron diffraction. In the absence of this information, computational and crystallographic studies implicate low frequency conrotary motions of the thiophene rings as well as motions orthogonal to the central carbon-carbon distance. Though the optical techniques employed in this study are only indirectly sensitive to the nuclear motions involved, we expect to provide a complete atomistic description of this classic conrotary ring closing reaction with conserved stereochemistry based on our femtosecond electron diffraction studies that are presently in progress. Direct observation of the nuclear motions involved in this process will give a complete understanding of the ultrafast dynamics associated with photoinduced electrocyclic reactions in diarylethene derivatives.

References

[1] Irie, M. *Chemical Reviews* **2000**, *100*, 1685-1716.

[2] Tian, H.; Yang, S. J. *Chemical Society Reviews* **2004**, *33*, 85-97.

[3] Irie, M.; Kobatake, S.; Horichi, M. *Science* **2001**, *291*, 1769-1772.

[4] Kobatake, S.; Takami, S.; Muto, H.; Ishikawa, T.; Irie, M. *Nature* **2007**, *446*, 778-781.

[5] Kobatake, S.; Irie, M. *Bulletin of the Chemical Society of Japan* **2004**, *77*, 195-210.

[6] Miyasaka, H.; Araki, S.; Tabata, A.; Nobuto, T.; Mataga, N.; Irie, M. *Chemical Physics Letters* **1994**, *230*, 249-254.

[7] Tamai, N.; Saika, T.; Shimidzu, T.; Irie, M. *Journal of Physical Chemistry* **1996**, *100*, 4689-4692.

[8] Miyasaka, H.; Nobuto, T.; Itaya, A.; Tamai, N.; Irie, M. *Chemical Physics Letters* **1997**, *269*, 281-285.

[9] Owrutsky, J. C.; Nelson, H. H.; Baronavski, A. P.; Kim, O. K.; Tsivgoulis, G. M.; Gilat, S. L.; Lehn, J. M. *Chemical Physics Letters* **1998**, *293*, 555-563.

[10] Ohtaka, N.; Hase, Y.; Uchida, K.; Irie, M.; Tamai, N. *Molecular Crystals and Liquid Crystals* **2000**, *344*, 83-88.

[11] Ern, J.; Bens, A. T.; Martin, H. D.; Mukamel, S.; Tretiak, S.; Tsyganenko, K.; Kuldova, K.; Trommsdorff, H. P.; Kryschi, C. *Journal of Physical Chemistry A* **2001**, *105*, 1741-1749.

[12] Ern, J.; Bens, A. T.; Martin, H. D.; Kuldova, K.; Trommsdorff, H. P.; Kryschi, C. *Journal of Physical Chemistry A* **2002**, *106*, 1654-1660.

[13] Hania, P. R.; Telesca, R.; Lucas, L. N.; Pugzlys, A.; van Esch, J.; Feringa, B. L.; Snijders, J. G.; Duppen, K. *Journal of Physical Chemistry A* **2002**, *106*, 8498-8507.

[14] Bertarelli, C.; Gallazzi, M. C.; Stellacci, F.; Zerbi, G.; Stagira, S.; Nisoli, M.; De Silvestri, S. *Chemical Physics Letters* **2002**, *359*, 278-282.

[15] Miyasaka, H.; Nobuto, T.; Murakami, M.; Itaya, A.; Tamai, N.; Irie, M. *Journal of Physical Chemistry A* **2002**, *106*, 8096-8102.

[16] Hania, P. R.; Pugzlys, A.; Lucas, L. N.; de Jong, J. J. D.; Feringa, B. L.; van Esch, J. H.; Jonkman, H. T.; Duppen, K. *Journal of Physical Chemistry A* **2005**, *109*, 9437-9442.

[17] Uchida, K.; Takata, A.; Ryo, S. I.; Saito, M.; Murakami, M.; Ishibashi, Y.; Miyasaka, H.; Irie, M. *Journal of Materials Chemistry* **2005**, *15*, 2128-2133.

[18] Tani, K.; Ishibashi, Y.; Miyasaka, H.; Kobatake, S.; Irie, M. *Journal of Physical Chemistry C* **2008**, *112*, 11150-11157.

[19] Okabe, C.; Nakabayashi, T.; Nishi, N.; Fukaminato, T.; Kawai, T.; Irie, M.; Sekiya, H. *Journal of Physical Chemistry A* **2003**, *107*, 5384-5390.

[20] Shim, S.; Eom, I.; Joo, T.; Kim, E.; Kim, K. S. *Journal of Physical Chemistry A* **2007**, *111*, 8910-8917.

[21] Ern, J.; Bens, A. T.; Bock, A.; Martin, H. D.; Kryschi, C. *Journal of Luminescence* **1998**, *76-7*, 90-94.

[22] Ern, J.; Bens, A. T.; Martin, H. D.; Mukamel, S.; Schmid, D.; Tretiak, S.; Tsiper, E.; Kryschi, C. *Chemical Physics* **1999**, *246*, 115-125.

[23] Miyasaka, H.; Murakami, M.; Itaya, A.; Guillaumont, D.; Nakamura, S.; Irie, M. *Journal of the American Chemical Society* **2001**, *123*, 753-754.

[24] Miyasaka, H.; Murakami, M.; Okada, T.; Nagata, Y.; Itaya, A.; Kobatake, S.; Irie, M. *Chemical Physics Letters* **2003**, *371*, 40-48.

[25] Shim, S. D.; Joo, T. H.; Bae, S. C.; Kim, K. S.; Kim, E. Y. *Journal of Physical Chemistry A* **2003**, *107*, 8106-8110.

[26] Murakami, M.; Miyasaka, H.; Okada, T.; Kobatake, S.; Irie, M. *Journal of the American Chemical Society* **2004**, *126*, 14764-14772.

[27] Ishibashi, Y.; Tani, K.; Miyasaka, H.; Kobatake, S.; Irie, M. *Chemical Physics Letters* **2007**, *437*, 243-247.

[28] Ishibashi, Y.; Mukaida, M.; Falkenstrom, M.; Miyasaka, H.; Kobatake, S.; Irie, M. *Physical Chemistry Chemical Physics* **2009**, *11*, 2640-2648.

[29] Ishibashi, Y.; Okuno, K.; Ota, C.; Umesato, T.; Katayama, T.; Murakami, M.; Kobatake, S.; Irie, M.; Miyasaka, H. *Photochemical & Photobiological Sciences* **2010**, *9*, 172-180.

[30] Yamada, T.; Kobatake, S.; Irie, M. *Bulletin of the Chemical Society of Japan* **2000**, *73*, 2179-2184.

[31] Yamada, T.; Muto, K.; Kobatake, S.; Irie, M. *Journal of Organic Chemistry* **2001**, *66*, 6164-6168.

[32] Miller, R. J. D.; Ernstorfer, R.; Harb, M.; Gao, M.; Hebeisen, C. T.; Jean-Ruel, H.; Lu, C.; Moriena, G.; Sciaini, G. *Acta Crystallographica Section A* **2010**, *66*, 137-156.

[33] Boggio-Pasqua, M.; Ravaglia, M.; Bearpark, M. J.; Garavelli, M.; Robb, M. A. *Journal of Physical Chemistry A* **2003**, *107*, 11139-11152.

[34] Wilhelm, T.; Piel, J.; Riedle, E. *Optics Letters* **1997**, *22*, 1494-1496.

[35] Dwyer, J. R.; Hebeisen, C. T.; Ernstorfer, R.; Harb, M.; Deyirmenjian, V. B.; Jordan, R. E.; Miller, R. J. D. *Philosophical Transactions of the Royal Society a-Mathematical Physical and Engineering Sciences* **2006**, *364*, 741-778.

[36] M. J. Frisch, G. W. T., H. B. Schlegel, G. E. Scuseria, ; M. A. Robb, J. R. C., G. Scalmani, V. Barone, B. Mennucci, ; G. A. Petersson, H. N., M. Caricato, X. Li, H. P. Hratchian, ; A. F. Izmaylov, J. B., G. Zheng, J. L. Sonnenberg, M. Hada, ; M. Ehara, K. T., R. Fukuda, J. Hasegawa, M. Ishida, T. Nakajima, ; Y. Honda, O. K., H. Nakai, T. Vreven, J. A. Montgomery, Jr., ; J. E. Peralta, F. O., M. Bearpark, J. J. Heyd, E. Brothers, ; K. N. Kudin, V. N. S., R. Kobayashi, J. Normand, ; K. Raghavachari, A. R., J. C. Burant, S. S. Iyengar, J. Tomasi, ; M. Cossi, N. R., J. M. Millam, M. Klene, J. E. Knox, J. B. Cross, ; V. Bakken, C. A., J. Jaramillo, R. Gomperts, R. E. Stratmann, ; O. Yazyev, A. J. A., R. Cammi, C. Pomelli, J. W. Ochterski, ; R. L. Martin, K. M., V. G. Zakrzewski, G. A. Voth, ; P. Salvador, J. J. D., S. Dapprich, A. D. Daniels, ; O. Farkas, J. B. F., J. V. Ortiz, J. Cioslowski, ; and D. J. Fox, G., Inc. Wallingford CT, 2009.

[37] Casida, M. E.; Jamorski, C.; Casida, K. C.; Salahub, D. R. *Journal of Chemical Physics* **1998**, *108*, 4439-4449.

[38] Shibata, K.; Muto, K.; Kobatake, S.; Irie, M. *Journal of Physical Chemistry A* **2002**, *106*, 209-214.

[39] Irie, M.; Lifka, T.; Kobatake, S.; Kato, N. *Journal of the American Chemical Society* **2000**, *122*, 4871-4876.

[40] Lucotti, A.; Bertarelli, C.; Zerbi, G. *Chemical Physics Letters* **2004**, *392*, 549-554.

[41] Irie, M.; Lifka, T.; Uchida, K.; Kobatake, S.; Shindo, Y. *Chemical Communications* **1999**, 747-748.

[42] Kobatake, S.; Yamada, M.; Yamada, T.; Irie, M. *Journal of the American Chemical Society* **1999**, *121*, 8450-8456.

[43] Irie, M.; Sakemura, K.; Okinaka, M.; Uchida, K. *Journal of Organic Chemistry* **1995**, *60*, 8305-8309.

[44] (44) Kobatake, S.; Morimoto, M.; Asano, Y.; Murakami, A.; Nakamura, S.; Irie, M. *Chemistry Letters* **2002**, 1224-1225.

[45] Irie, M.; Miyatake, O.; Uchida, K. *Journal of the American Chemical Society* **1992**, *114*, 8715-8716.

[46] Jean-Ruel, H.; Gao, M.; Cooney, R. R.; Lu, C.; Sciaini, G.; Moriena, G.; Miller, D. R. In *Ultrafast Phenomena XVII: Proceedings of the 17th International Conference*; Oxford University Press, Inc.: 2010, p 337-339.

[47] Goldberg, A.; Murakami, A.; Kanda, K.; Kobayashi, T.; Nakamura, S.; Uchida, K.; Sekiya, H.; Fukaminato, T.; Kawai, T.; Kobatake, S.; Irie, M. *Journal of Physical Chemistry A* **2003**, *107*, 4982-4988.

[48] Uchida, K.; Guillaumont, D.; Tsuchida, E.; Mochizuki, G.; Irie, M.; Murakami, A.; Nakamura, S. *Journal of Molecular Structure-Theochem* **2002**, *579*, 115-120.

[49] Patel, P. D.; Masunov, A. E. *Journal of Physical Chemistry A* **2009**, *113*, 8409-8414.

[50] Sauer, P.; Allen, R. E. *Chemical Physics Letters* **2007**, *434*, 260-264.

[51] Asano, Y.; Murakami, A.; Kobayashi, T.; Goldberg, A.; Guillaumont, D.; Yabushita, S.; Irie, M.; Nakamura, S. *Journal of the American Chemical Society* **2004**, *126*, 12112-12120.

[52] Guillaumont, D.; Kobayashi, T.; Kanda, K.; Miyasaka, H.; Uchida, K.; Kobatake, S.; Shibata, K.; Nakamura, S.; Irie, M. *Journal of Physical Chemistry A* **2002**, *106*, 7222-7227.